Archives of Mechanics • Archiwum Mechaniki Stosowanej • 29, 4, pp. 561–591, Warszawa 1977

Mathematical elaboration of the double sliding, free rotating model(*)

G. DE JOSSELIN DE JONG (DELFT)

THE PAPER is devoted to the theoretical foundations and development of a rigid-perfectly plastic model describing the flow of an ideally granular medium. The main idea of the approach, suggested by the author in 1958, is the coincidence of slip lines with planes on which the yield condition appropriate for granular media takes the form of a friction law. As a consequence of such an assumption, the principal directions of strain rate and stress tensors may deviate. In addition, a non-uniquess of the solution of boundary value problems results, the only restriction on the solution being imposed by the condition of energy dissipation. The paper brings a discussion of basic assumptions, an analysis of the type of governing differential equations and properties of discontinuity lines in velocities, and a description of a technique of constructing the velocity field with the respective restrictions imposed on this field.

Praca poświęcona jest podstawom teoretycznym i opisom matematycznym pewnego modelu ciała sztywno-idealnie plastycznego opisującego płaskie płynięcie ośrodka idealnie sypkiego. Istotą tego modelu, zaproponowanego przez autora w 1958 r., jest pokrywanie się linii poślizgu z płaszczyznami, na których obowiązujący dla ośrodków sypkich warunek plastyczności Coulomba przyjmuje postać prawa tarcia. Konsekwencją takiej kinematyki jest możliwość niepokrywania się kierunków głównych tensorów naprężenia i prędkości odkształcenia oraz niejednoznaczność rozwiązania zagadnienia brzegowego, ograniczonego jedynie przez pewne nierówności o charakterze termodynamicznym. W pracy przedstawiono założenia modelu, analizę typu opisujących go równań różniczkowych, własności linii nieciągłości prędkości oraz metodę budowy pola prędkości i jego ograniczeń.

Работа посвящена теоретическим основам и математическим описаниям некоторой модели идеально-жёткого пластического тела, описывающей плоское течение идеально сыпучей среды. Суть этой модели, предложенной автором в 1958 году, заключается в совпадении линии скольжения с плоскостями, для которых условие пластичности Кулона для сыпучих сред, принимает вид закона трения. Результатом такой кинематики является возможность несовпадения направлений главных осей тензоров напряжения и скорости деформации, а также неоднозначности решения краевой задачи, ограниченной только некоторыми неравенствами, имеющими термодинамический характер. В работе представлены основные положения, касающиеся модели, анализ дифференциальных уравнений, описывающих эту модель, свойства линий разрыва скорости, а также метод построения поля скоростей и его ограничений.

Introduction

THE PURPOSE of the double sliding, free rotating model is to represent the flow behaviour of a granular assembly in such a simplified form, that it becomes amenable to mathematical treatment. A real granular medium possesses a kinematic behaviour defying mathematical description because it consists of a vast amount of discrete particles arranged in an intricate, random way. Instead of trying to simplify the combined motions of these particles by an analysis of approximations, the model was developed on the basis of the following con-

(*) Paper presented at the Euromech Colloqium 84 in "Mechanics of Granular Materials", Warsaw, July 1976.

ceptual assumptions. A granular mass flows, as if it were subdivided in conglomerates that slide with respect to each other along the division planes. The orientation of the planes is assumed to be such that they are the planes on which the available shear resistance is exhausted by the shear stress. In the case of planes train flow these planes intersect the relevant x, y-plane perpendicularly along lines, coinciding with the two conjugate stress characteristics.

Since Coulomb (1773) introduced the concept of an internal friction angle ϕ and sliding planes, the idea to generalize the flow behaviour in the manner mentioned above has occurred to several investigators.

MANDEL (1947) studied the mechanism of sliding units and deduced two of the four relevant differential equations. In a later publication (MANDEL, 1966) he considered the system of equations to be void (French: vide) because the rotation, that has to be added to the two possible sliding modes, renders the system indeterminate.

GENIEV (1958) developed equations for a single sliding model. In this model sliding in a point can only occur in one of the two conjugate directions. It seems logical to adopt this assumption because it is difficult to visualize two conjugate slidings of different magnitude to occur simultaneously at a point. This model will be indicated below as the *single sliding model*. It can be shown that the stress and strain rate tensors are not coaxial in this model, and that a deviation of $+\frac{1}{2}\phi$, respectively $-\frac{1}{2}\phi$, exists for the two different modes of sliding.

A double sliding model was proposed by DE JOSELIN DE JONG (1958), because it was considered necessary to account for the occurrence of two slidings in the two conjugate directions at a point, developing one after the other. The total effect of two of those successive motions is a double sliding which, mathematically, is introduced as occurring simultaneously. Denying the model this double sliding amounts in over-estimating its internal resistance against possible flow patterns.

It was concluded that the model generates noncoaxiality of stress and strain-rate tensors with a possible deviation angle varying from $-\frac{1}{2}\phi$ to $+\frac{1}{2}\phi$. Coaxiality is admitted as one of the possible modes of flow, but the flow behaviour is not limited to it. Noncoaxiality was observed and reported by DRESCHER et al. (1972) in a photoelastic disc assembly, which can be considered as a two-dimensional analogue of a granular medium.

Freedom of rotation of the sliding units and the thermodynamic requirement of energy dissipation were introduced (DE JOSSELIN DE JONG, 1959) in developing a graphical procedure for solving boundary value problems. The model was called the *double sliding, free rotating model* (DE JOSSELIN DE JONG, 1971 a).

SPENCER (1964), ZAGAINOV (1967) and MANDL et al. (1970) developed first-order differential equations for the velocities of a double sliding model. In their analyses the rotation is restricted and assumed to be a known quantity, related to the rotation of the stress tensor. As pointed out by MANDEL (1966) there exists no physical law requiring such a relationship and it was demonstrated (DRESCHER et al., 1972) that in a photoelastic disc assembly the two rotations can be opposite (*). By prohibiting the rotation to develop

(*) A similar result was observed by DRESCHER (1976) in tests on optically sensitive glass particles.

freely, an irrealistic resistance is built into the model. This model will be called the *non-free rotating model.*

The constitutive flow rules for the double sliding, free rotating model were developed (DE JOSSELIN DE JONG, 1971 a) by expressing the shear strain rates and the structural rotation in the derivatives of the velocity components. After introducing the thermodynamic requirement of energy dissipation and the assumption of freedom of rotation, the flow rule reduces to one equation and two inequalities. Because of the double sliding and the freedom of rotation there are three relations and as a consequence solutions of boundary value problems are nonunique. Because of the thermodynamic requirement, however, the class of possible solutions is bounded and the system is not unrestricted as suggested by MANDEL (1966). In the hodograph plane the class of solutions is represented by a region, bounded by four enclosing lines, valid for the velocity in a point. The boundary value problem relevant here is to determine the velocity distribution in a field with a known limit stress state and the velocities given on the boundary.

In not giving unique answers to certain boundary value problems the double sliding model resembles the single sliding model, for which the solutions consists of two diametrical points of the four-sided region in the hodograph. The solution is reduced to two points because that model has more internal resistance built into it. Still more resistance is introduced by the coaxial and non-free rotating models which have unique points as solution.

The lack of uniqueness of solutions was considered (MRÓZ, 1975) to be an indication that the flow rule of the double sliding, free rotating model is "incomplete". It is the opinion of this author, that completing the system by introducing limiting conditions on the local behaviour in the interior has the effect of introducing internal resistances. This results in overestimating the strength of a grain assembly. If prediction of a real behaviour has to result in a unique velocity distribution, additional conditions on the boundaries are to be imposed. An example of such an additional condition is e.g. the minimalization of the horizontal normal stress in the case of simple shear, which leads (DE JOSSELIN DE JONG, 1971 b) to the prediction of a tilting bookrow mechanism.

It may be mentioned here that the flow rule as developed for the double sliding, free rotating model differs from those for the other models by including the thermodynamic requirement of energy dissipation. Although often not pointed out explicity, solutions have to be verified also for the other models afterwards so as not to violate this requirement. Such a verification is sometimes neglected, an omission that is avoided when the requirement is introduced a priori.

In the double sliding, free rotating model the rotation of the slices is free in the sense that it is not restricted by conditions at a point. The rotation, however, is not entirely free because the motions of sliding slices must be such, that compatibility of adjacent regions is preserved. The requirements of compatibility are expressed (DE JOSSELIN DE JONG, 1974) by second-order differential equations in the velocity components, which lead to two relations between the derivatives of the shear strain rates and the structural rotation. Physically these relations can be interpreted in terms of bending of the sliding slices.

In developing the double sliding, free rotating model mathematically, the sliding slices are introduced as being internally rigid. This may suggest that the slices are to be considered

also as not being able to bend. There is some advantage mathematically to introduce rigidity against bending, because the compatibility relations then provide additional information which can be used to "complete" the system in the sense that non-uniqueness of solutions is reduced.

The opinion of this author is, that completing the system by introducing rigidity against bending is tantamount to attributing the model an internal resistance that may be irrealistic. The sliding slices represent grain conglomerates which derive their internal resistance from the contact forces. The latter keep the non-sliding particles together. When the slices are slender and contain many particles, these internal forces may not be effective enough to prevent also bending. In order to avert overestimation of resistance built into the model, it is preferred to consider the model to be flexible with respect to bending.

It has not yet been verified experimentally how much rigidity or flexibility, with respect to bending, occurs in granular assemblies. A manner to investigate this is to consider the thickness of bands along which large variations in velocity occur, and the directions of strong velocity discontinuities. Since the connection between slice flexibility and discontinuity direction has not been published previously, this aspect is treated in some detail in this presentation. If the conclusion from experiments is that bending must be taken into account, the name of the model should become the *double sliding, free rotating, flexible model.*

In this article, especially the double sliding, free rotating model is treated and mathematical expressions that describe its behaviour are derived. The reason to prefer this model to the other ones mentioned above is that the difference between properties attributed to them can be shown to amount to built-in resistances. For an engineer who wants to avoid overestimation of strength of his building materials, the weakest model is preferable.

The model is based on simplifications and it is not claimed to represent an exact rendering of the behaviour of granular media. It is, however, interesting to investigate what a model that incorporates the typical aspect of internal friction primarily will do, and to predict its behaviour by applying well-known laws of physics.

The model is originally divised for the motions in continuous flow of granular assemblies consisting of rigid particles, under conditions of constant stress and constant volume. It is possible to extend the formulae to the case of dilatancy by introducing an uplift angle θ in the sliding planes. Since only small variations in the equations are involved, these are mentioned at the end of each chapter. The model can also be used for describing the behaviour of rock masses that are subdivided into subunits by a preliminary fissuring process and move subsequently by sliding of the units with respect to each other along the fissures. These fissures then replace the planes of maximum stress obliquity as potential sliding planes. In the case of rocks, resistance against bending could be encountered and the possibility of completing the system by using the compatibility relations may be envisaged.

In order to give a consistent treatment the basic relations describing the model behaviour are derived in terms of the components of the velocity gradient tensor in Chapter 1. In Chapter 2 the character of this system of relations is analyzed by comparing its properties to properties known to exist for hyperbolic systems. In Chapter 3 the velocity discontinuities are considered.

1. Development of basic constitutive relations

1.1. Sliding slices model, definition of a, b and Ω

The double sliding, free rotating model for granular assemblies in progressive flow consists of separation planes coinciding with the planes of maximum stress obliquity along which sliding occurs exclusively. The model is based on the assumption that in a real granular medium at limit stress state, sliding will occur along those planes where the shear resistance is exhausted. In the case of plane strain these planes intersect the relevant x, y plane perpendicularly along the stress characteristics: s^1, s^2 which are, in general, curved lines (Fig. 1). The angles of s^1, s^2 with the x-axis, are respectively α_1, α_2 given by

$$\begin{aligned} \alpha_1 &= \psi - \frac{1}{4}\pi - \frac{1}{2}\phi, \\ \alpha_2 &= \psi + \frac{1}{4}\pi + \frac{1}{2}\phi, \end{aligned} \tag{1.1}$$

where ψ—angle between x-axis and minor principal compression stress, σ_3^1 and ϕ—angle of internal friction of the material.

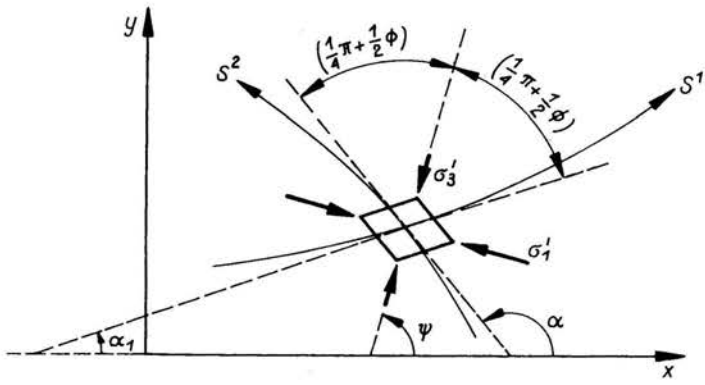

FIG. 1. S^1 and S^2 are the stress characteristics at angles $\pm\left(\frac{1}{4}\pi+\frac{1}{2}\phi\right)$ with σ_3', the minor principal compression stress.

The stress state is considered to have been established preliminary, so the angle ψ is a known function of x and y. The angle ϕ is considered to be a constant in the field. The angle between s^1 and s^2 lines is then everywhere: $(\alpha_2-\alpha_1) = \frac{1}{2}\pi+\phi = \text{constant}$.

If the model is to represent the limit state when sliding occurs under conditions of constant volume, the sliding planes are smooth in order to guarantee that volume is conserved during sliding. Because of the smoothness of the planes the relative velocity of two adjacent slices is a vector which is parallel to the separation plane between slices. In Fig. 2, left and right, the relative velocity vectors are $d\mathbf{V}_a$ and $d\mathbf{V}_b$.

The sliding motion is restricted to a relative displacement of adjacent slices in such a direction that the shear stresses on the planes (see Fig. 2, centre) dissipate energy. This restriction is due to the friction character of the behaviour of granular media and is called here the "thermodynamic requirement of energy dissipation".

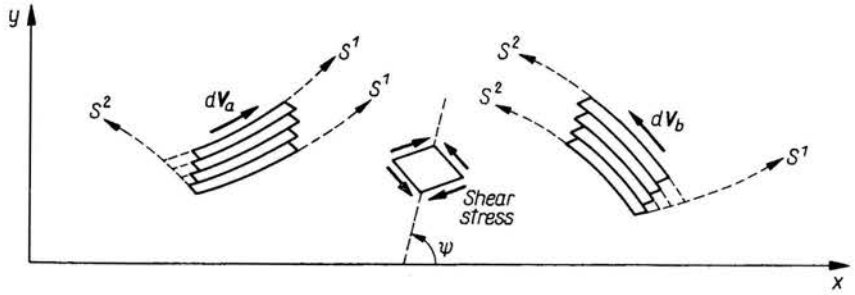

FIG. 2. The sliding planes coincide with the stress characteristics. Sliding is in the direction of the shear stresses on the sliding planes.

No other restrictions are imposed on the motion of the slices in the model. Slidings are left free to adopt any magnitude. In the two conjugate stress-characteristic directions slidings can develop concurrently and can posses unequal values.

Further, it is assumed that the rotation of the slices is free to adopt any magnitude desired. The slice rotation is called "structural" rotation here because it is the rotation of the grain structure. This rotation differs from the asymmetric part of the velocity gradient tensor which generally is called the material rotation. This is so because it represents the rotation of the grain material as a total when considered as a deformable body from the outside.

In order to describe sliding of the slices mathematically, the discontinuous motion, encountered when blocks of finite size slide with respect to each other along discrete separation planes, is replaced by a continuous velocity distribution. Mathematically the slices are replaced by sheets of infinitesimal thickness, like pages of a book. These sheets intersect the x, y-plane along lines in s^1, s^2-directions. Scalar quantities a, b are introduced; their values indicate the strength of sliding along s^1, s^2-lines respectively, defined by

a—shear strain rate, created by slidings in s^1-direction, such that the relative velocity $d\mathbf{V}_a$ of two adjacent s^1-lines is equal to a multiplied by their mutual perpendicular distance (Fig. 2, left);

b—shear strain rate, created by slidings in s^2-direction such that the relative velocity $d\mathbf{V}_b$ of two adjacent s^2-lines is equal to b multiplied by their mutual perpendicular distance (Fig. 2, right).

The quantities a, b are defined to be positive when sliding is as in Fig. 2. In order to satisfy the thermodynamic requirement of energy dissipation, the scalar quantities a, b are then restricted to positive values or

$$0 \leqslant a \leqslant +\infty, \quad 0 \leqslant b \leqslant +\infty. \tag{1.2}$$

The double sliding mechanism admits unequal sliding rates in conjugate directions or

$$0 \leqq (a/b) \leqq +\infty. \tag{1.3}$$

The magnitude of structural rotation is indicated by a scalar quantity Ω, positive for counterclockwise rotation (Fig. 3). This rotation is superimposed on the slidings and occurs in a manner such that slices are not deformed internally. The superimposed rotation has therefore the character of a rigid body rotation. The freedom of rotation is expressed mathematically as

$$-\infty \leqq \Omega \leqq +\infty. \tag{1.4}$$

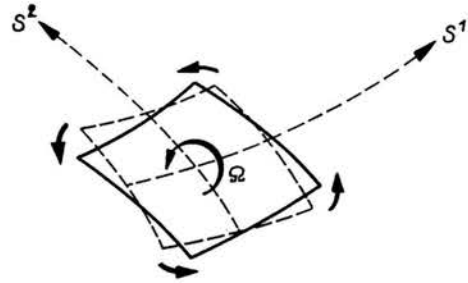

FIG. 3. Structural rotation Ω positive for counterclockwise rotation.

The inequalities (1.2) and (1.4) are a mathematical formulation of the requirements, imposed by physical considerations on the flow mechanism. The scalars a, b and Ω are finite quantities, when the velocity distribution is continuous. In the expressions (1.2) and (1.4) the case that a, b and Ω might be infinite is also included. Physically there is no objection to infinite values and mathematically they form the possibility to include strong velocity discontinuitues in the flow rule. These are created when blocks of finite size slide with respect to each other along discrete separation planes.

1.2. Velocity gradient tensor

The flow rule of the double sliding, free rotating model can be expressed in terms of the components of the velocity gradient tensor. The rule is developed by expressing the shear strain rates a, b and the structural rotation Ω in terms of these components and then applying the physical requirements, Eqs. (1.2) and (1.4).

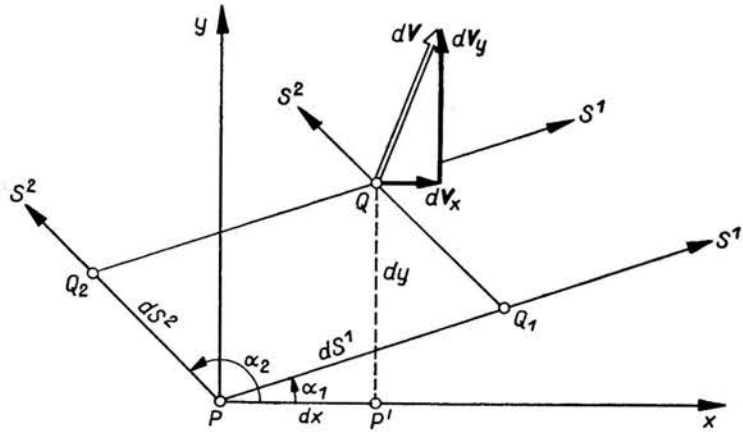

FIG. 4. Relative velocity $d\mathbf{V}$ of points P and Q at infinitesimal distance.

Let V_x, V_y be the components of the velocity $\mathbf{V}$ of a point P and let dV_x, dV_y be the components of the relative velocity $d\mathbf{V}$ of a point Q with respect to the point P (Fig. 4). Let the infinitesimal distance between P and Q be given by its components $PP' = dx$ and $P'Q = dy$. The relative velocity components can then be written as total differentials by using the partial covariant derivatives $V_{x,x}$ ... etc. as

$$\begin{aligned} dV_x &= V_{x,x}dx + V_{x,y}dy, \\ dV_y &= V_{y,x}dx + V_{y,y}dy. \end{aligned} \tag{1.5}$$

The s^2-line through Q intersects the s^1-line through P at point Q_1 (Fig. 4), located at an infinitesimal distance ds^1 from P. In the same manner: Q_2, at the distance ds^2 from P, is the intersection of the s^1 through Q and the s^2 through P. From Fig. 4 it follows that

$$\begin{aligned} dx &= ds^1 \cos\alpha_1 + ds^2 \cos\alpha_2, \\ dy &= ds^1 \sin\alpha_1 + ds^2 \sin\alpha_2 \end{aligned} \tag{1.6}$$

giving inversely with Eq. (1.1)

$$\begin{aligned} ds^1 \cos\phi &= +dx\sin\alpha_2 - dy\cos\alpha_2, \\ ds^2 \cos\phi &= -dx\sin\alpha_1 + dy\cos\alpha_1. \end{aligned} \tag{1.7}$$

The relative velocity of Q with respect to P consists of three components: $d\mathbf{V}_a$, $d\mathbf{V}_b$, $d\mathbf{V}_\Omega$ which are respectively due to a, b and Ω (see Fig. 5).

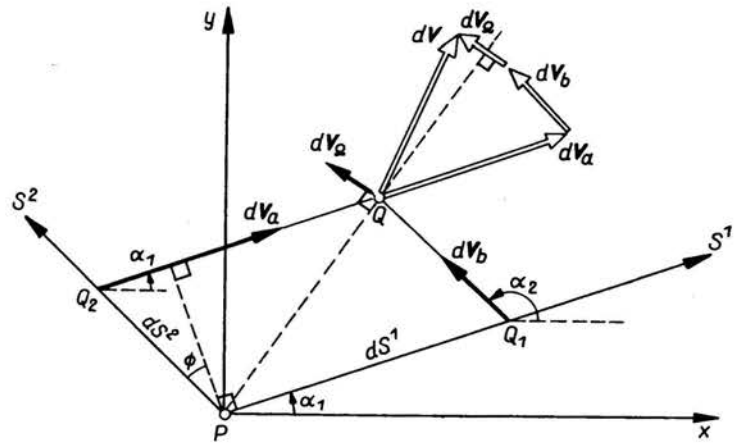

FIG. 5. Relative velocity $d\mathbf{V}$ consists of components, due to the shear strain rates a, b and the structural rotation Ω.

Shear strain rate, a. The relative velocity of the two s^1-lines through P and Q as created by the shear strain rate a is equal to a multiplied by the perpendicular distance of the two s^1-lines. The distance is equal to $ds^2\cos\phi$, see Fig. 5, because $\alpha_2 - \alpha_1 = \frac{1}{2}\pi + \phi$.

Therefore the relative velocity component $d\mathbf{V}_a$ has, with (1.7), a magnitude equal to

$$|d\mathbf{V}_a| = a\,ds^2\cos\phi = -a\sin\alpha_1\,dx + a\cos\alpha_1\,dy.$$

In the case of continuing flow at constant volume, the separation planes are smooth and the direction of $d\mathbf{V}_a$ is parallel to the s^1-lines. Then, its components in x, y directions are

$$\begin{aligned}(dV_a)_x &= |d\mathbf{V}_a|\cos\alpha_1 = -a\sin\alpha_1\cos\alpha_1\,dx + a\cos^2\alpha_1\,dy,\\ (dV_a)_y &= |d\mathbf{V}_a|\sin\alpha_1 = -a\sin^2\alpha_1\,dx + a\cos\alpha_1\sin\alpha_1\,dy.\end{aligned} \tag{1.8}$$

Shear strain rate, b. In the same manner $d\mathbf{V}_b$, the relative velocity of Q with respect to P as created by the shear strain rate b, has a magnitude

$$|d\mathbf{V}_b| = b\,ds^1\cos\phi = +b\sin\alpha_2\,dx - b\cos\alpha_2\,dy$$

and being parallel to the s^2-lines its components are

$$\begin{aligned}(dV_b)_x &= |d\mathbf{V}_b|\cos\alpha_2 = +b\sin\alpha_2\cos\alpha_2\,dx - b\cos^2\alpha_2\,dy,\\ (dV_b)_y &= |d\mathbf{V}_b|\sin\alpha_2 = +b\sin^2\alpha_2\,dx - b\cos\alpha_2\sin\alpha_2\,dy.\end{aligned} \tag{1.9}$$

Structural rotation, Ω. In addition to the sliding motions the parallelogram PQ_1QQ_2 is able to rotate as a rigid body with a structural rotation Ω. The relative velocity $d\mathbf{V}_\Omega$ of Q with respect to P is then perpendicular to the line PQ and has a magnitude of Ω multiplied by the distance PQ (Fig. 5). Its components in x, y-directions are then

$$\begin{aligned}(dV_\Omega)_x &= -\Omega\,dy,\\ (dV_\Omega)_y &= +\Omega\,dx.\end{aligned} \tag{1.10}$$

Relative velocity, $d\mathbf{V}$. The total relative velocity $d\mathbf{V}$ of Q with respect to P is the vector summation of the three relative velocities created by a, b and Ω (Fig. 5), and their x, y-components are therefore related by

$$\begin{aligned}dV_x &= (dV_a)_x + (dV_b)_x + (dV_\Omega)_x,\\ dV_y &= (dV_a)_y + (dV_b)_y + (dV_\Omega)_y.\end{aligned} \tag{1.11}$$

By using Eqs. (1.8), (1.9), (1.10) the components dV_x and dV_y can be expressed in terms containing dx and terms containing dy. By comparing these terms, with corresponding terms in Eqs. (1.5), the following relations result:

$$\begin{aligned}V_{x,x} &= -a\sin\alpha_1\cos\alpha_1 + b\sin\alpha_2\cos\alpha_2,\\ V_{x,y} &= +a\cos^2\alpha_1 - b\cos^2\alpha_2 - \Omega,\\ V_{y,x} &= -a\sin^2\alpha_1 + b\sin^2\alpha_2 + \Omega,\\ V_{y,y} &= +a\cos\alpha_1\sin\alpha_1 - b\cos\alpha_2\sin\alpha_2.\end{aligned} \tag{1.12}$$

Solving these relations for a, b and Ω gives

$$\begin{aligned}a\sin 2\phi &= +(V_{x,x}-V_{y,y})\sin(2\psi+\phi) - (V_{x,y}+V_{y,x})\cos(2\psi+\phi),\\ b\sin 2\phi &= -(V_{x,x}-V_{y,y})\sin(2\psi-\phi) + (V_{x,y}+V_{y,x})\cos(2\psi-\phi),\\ 2\Omega\sin\phi &= +(V_{x,x}-V_{y,y})\sin 2\psi - (V_{x,y}+V_{y,x})\cos 2\psi + (-V_{x,y}+V_{y,x})\sin\phi.\end{aligned} \tag{1.13}$$

By adding the first and last of Eqs. (1.12) the result is

$$V_{x,x} + V_{y,y} = 0. \tag{1.14}$$

Equation (1.14) shows that sliding occurs under conditions of constant volume, because the left hand side represents the divergence of $\mathbf{V}$.

The system of four equations, Eqs. $(1.13)_1$ with (1.14), are the basic relations describing the flow mechanism of the double sliding, free rotating model. They express the scalars a, b (the magnitudes of the shear strain rates) and Ω (the magnitude of the structural rotation) in terms of the components of the velocity gradient tensor. Together with the restrictions in Eqs. (1.2) and (1.4) imposed on the scalars a, b and Ω they form the constitutive relations of the model.

1.3. Dilatancy

The model can be made to represent the case of dilatancy when sliding is accompanied by volume changes. This is achieved by assuming the sliding planes not to be smooth, but having protuberances which create an uplift motion during sliding (see Fig. 6). These protuberances are visualized as staircase steps or saw teeth which have an angle θ with the average direction α^* of a sliding plane. Sliding occurs along the faces of the steps, so that the relative velocity component $d\mathbf{V}_a^*$ between two lines in α^* direction has a direction $(\alpha^*+\theta)$ with the x-axis (see Fig. 6). There are two possible sliding directions and it is assumed here that an uplift angle of the same magnitude θ is active in both conjugate directions.

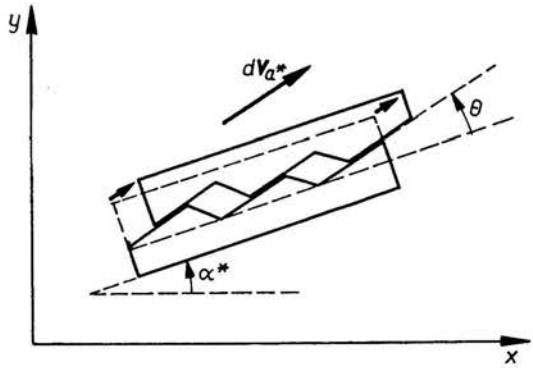

FIG. 6. Sliding with uplift over planes with protuberances at angle θ.

Such a model was introduced for dense sand in pre-failure state by NEWLAND and ALLELY (1957) and extended to the double sliding case by DE JOSSELIN DE JONG (1959). The tooth-shaped sliding planes were used by ROWE (1962, 1969) to develop dilatancy relations assuming that the inclination of the forces, transmitted by the teeth, is such as to exhaust the physical friction angle φ_μ of the particle material. He considered the coaxial case and, using a minimum energy ratio principle, he obtained relations which reduce for plane strain conditions when $\dot{\varepsilon}_2 = 0$ to the following system:

$$R = \frac{\sigma_1'}{\sigma_3'} = \operatorname{tg}\left(\frac{1}{4}\pi + \frac{1}{2}\phi^*\right)\operatorname{tg}\left(\frac{1}{4}\pi + \frac{1}{2}\varphi_\mu\right),$$

(1.15)

$$D = \frac{\dot{\varepsilon}_3}{-\varepsilon_1} = \operatorname{tg}\left(\frac{1}{4}\pi + \frac{1}{2}\phi^*\right)\operatorname{tg}\left(\frac{1}{4}\pi - \frac{1}{2}\varphi_\mu\right),$$

where σ_1' and σ_3'—major and minor principal compression stress, $\dot{\varepsilon}_1$ and $\dot{\varepsilon}_3$—principal

strain rates, $\frac{1}{4}\pi+\frac{1}{2}\phi^*$—angle between the sliding planes and the plane of the major principal compression stress.

It was shown (DE JOSSELIN DE JONG, 1976) that the same relations result by using exclusively the rules of friction and that the system (1.15) is not necessarily restricted to the case of coaxiality. For the noncoaxial case the relations keep the same form if D is not expressed in terms of principle strain rates $\dot{\varepsilon}_1$, $\dot{\varepsilon}_3$, but in $\dot{\varepsilon}(\sigma_1')$, $\dot{\varepsilon}(\sigma_3')$ the linear strain rates of lines in the directions of the principle stresses, σ_1' and σ_3', respectively. In order to make this distinction a quantity D^* was introduced, defined by

$$D^* = \dot{\varepsilon}(\sigma_3')/-\dot{\varepsilon}(\sigma_1'). \tag{1.16}$$

The system then is

$$\begin{aligned} R &= \operatorname{tg}\left(\frac{1}{4}\pi+\frac{1}{2}\phi^*\right)\operatorname{tg}\left(\frac{1}{4}\pi+\frac{1}{2}\varphi_\mu\right), \\ D^* &= \operatorname{tg}\left(\frac{1}{4}\pi+\frac{1}{2}\phi^*\right)\operatorname{tg}\left(\frac{1}{4}\pi-\frac{1}{2}\varphi_\mu\right). \end{aligned} \tag{1.17}$$

The angle ϕ^* introduced above in (1.15) in connection to the direction of the sliding planes differs from the angle of internal friction, ϕ, introduced in the previous analysis here. The difference is that previously, the sliding planes were the planes in which the shear resistance (as an average) was exhausted, while here the shear resistance is exhausted on the faces of the steps which make an angle θ with the sliding planes. Therefore the angle ϕ^* differs from φ, the current angle of maximum stress obliquity defined by

$$\sin\varphi = \frac{\sigma_1'-\sigma_3'}{\sigma_1'+\sigma_3'} = \frac{R-1}{R+1}. \tag{1.18}$$

The relation existing between ϕ^* and φ is developed at the end of this section.

Let α_1^* and α_2^* be the angles between the sliding planes s^{1*}, s^{2*} and the x-axis. Then, analogous to Eqs. (1.1), we have here

$$\begin{aligned} \alpha_1^* &= \psi-\frac{1}{4}\pi-\frac{1}{2}\phi^*, \\ \alpha_2^* &= \psi+\frac{1}{4}\pi+\frac{1}{2}\phi^*. \end{aligned} \tag{1.19}$$

Because of the teeth at an angle θ with s^{1*}, the direction of the relative velocity $d\mathbf{V}_{a*}$ of two slices separated by an s^{1*}-line makes an angle $(\alpha_1^*+\theta)$ with the x-axis (see Fig. 7). In the same manner the relative velocity $d\mathbf{V}_{b*}$ has a direction given by $(\alpha_2^*-\theta)$, (Fig. 7). So their x, y-components are

$$\begin{aligned} (dV_{a*})_x &= |d\mathbf{V}_{a*}|\cos(\alpha_1^*+\theta), \qquad (dV_{b*})_x = |d\mathbf{V}_{b*}|\cos(\alpha_2^*-\theta), \\ (dV_{a*})_y &= |d\mathbf{V}_{a*}|\sin(\alpha_1^*+\theta), \qquad (dV_{b*})_y = |d\mathbf{V}_{b*}|\sin(\alpha_2^*-\theta). \end{aligned}$$

Scalar quantities a^*, b^* are introduced in order to specify the magnitudes of the dilatant shear strain rate, created by the slidings, by the following definition: a^*, b^*—magnitude of the relative velocity created by the sliding of adjacent s^{1*}, s^{2*}-lines, respectively, divided by their mutual distance.

Then we have

$$|d\mathbf{V}_{a^*}| = a^* ds^{2*} \cos\phi^*, \quad |d\mathbf{V}_{b^*}| = b^* ds^{1*} \cos\phi^*$$

and the analysis of Sect. 1.2 gives for the components of the velocity gradient tensor

$$\begin{aligned} V_{x,x} &= -a^* \sin\alpha_1^* \cos(\alpha_1^* + \theta) + b^* \sin\alpha_2^* \cos(\alpha_2^* - \theta), \\ V_{x,y} &= +a^* \cos\alpha_1^* \cos(\alpha_1^* + \theta) - b^* \cos\alpha_2^* \cos(\alpha_2^* - \theta) - \Omega, \\ V_{y,x} &= -a^* \sin\alpha_1^* \sin(\alpha_1^* + \theta) + b^* \sin\alpha_2^* \sin(\alpha_2^* - \theta) + \Omega, \\ V_{y,y} &= +a^* \cos\alpha_1^* \sin(\alpha_1^* + \theta) - b^* \cos\alpha_2^* \sin(\alpha_2^* - \theta). \end{aligned} \tag{1.20}$$

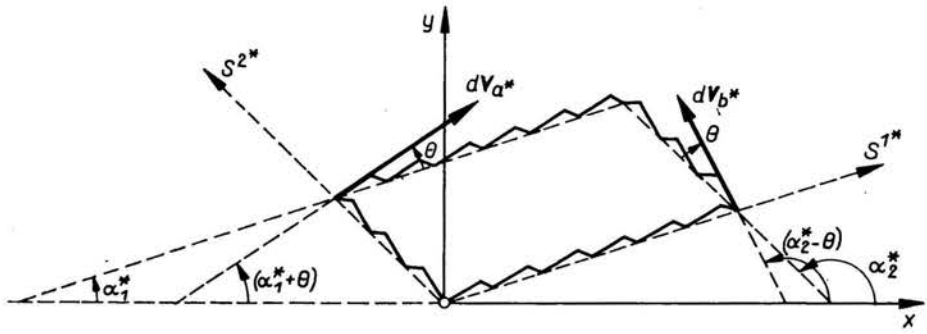

FIG. 7. Relative velocities $d\mathbf{V}_a^*$ and $d\mathbf{V}_b^*$ at angles θ with sliding planes.

Solving these relations for a^*, b^* and Ω gives

$$\begin{aligned} a^* \sin 2(\phi^* - \theta) &= +(V_{x,x} - V_{y,y}) \sin(2\psi + \phi^* - \theta) - (V_{x,y} + V_{y,x}) \cos(2\psi + \phi^* - \theta), \\ b^* \sin 2(\phi^* - \theta) &= -(V_{x,x} - V_{y,y}) \sin(2\psi - \phi^* + \theta) + (V_{x,y} + V_{y,x}) \cos(2\psi - \phi^* + \theta). \\ 2\Omega \sin(\phi^* - \theta) &= [(V_{x,x} - V_{y,y}) \sin 2\psi - (V_{x,y} + V_{y,x}) \cos 2\psi] \cos\theta \\ &\quad + (-V_{x,y} + V_{y,x}) \sin(\phi^* - \theta). \end{aligned} \tag{1.21}$$

By adding the first and last of Eqs. (1.20) it follows that

$$(a^* + b^*) \sin\theta = V_{x,x} + V_{y,y} \tag{1.22}$$

which expresses the rate of volume change in terms of the shear strain rates and the uplift angle. By adding Eqs. $(1.21)_1$ and $(1.21)_2$ it is deduced that

$$(a^* + b^*) \cos(\phi^* - \theta) = (V_{x,x} - V_{y,y}) \cos 2\psi + (V_{x,y} + V_{y,x}) \sin 2\psi. \tag{1.23}$$

Elimination of $(a^* + b^*)$ from the above two equations gives

$$(V_{x,x} + V_{y,y}) \cos(\phi^* - \theta) - [(V_{x,x} - V_{y,y}) \cos 2\psi + (V_{x,y} + V_{y,x}) \sin 2\psi] \sin\theta = 0. \tag{1.24}$$

The system of equations (1.21) and (1.24) reduces to the system of equations (1.13) and (1.14) when θ vanishes. From Fig. 1 it follows that the x-axis of coordinates is oriented in the direction of the major principal compression stress σ_1' when ψ is given the value $\frac{1}{2}\pi$. Then, Eq. (1.23) becomes

$$(a^* + b^*) \cos(\phi^* - \theta) = -V_{x,x} + V_{y,y}. \tag{1.25}$$

Since for that case $V_{x,x}$, $V_{y,y}$ are the linear strain rates of lines in the principal stress directions, we have

$$V_{x,x} = \dot{\varepsilon}(\sigma_1'), \quad V_{y,y} = \dot{\varepsilon}(\sigma_3'), \tag{1.26}$$

$$D^* = V_{y,y}/(-V_{x,x}).$$

Using Eqs. (1.22) and (1.25) it is then found that

$$D^* = \frac{\cos(\phi^*-\theta)+\sin\theta}{\cos(\phi^*-\theta)-\sin\theta} = \operatorname{tg}\left(\frac{1}{4}\pi+\frac{1}{2}\phi^*\right)\operatorname{tg}\left(\frac{1}{4}\pi-\frac{1}{2}\phi^*+\theta\right).$$

By multiplying the relations (1.17) it follows that

$$RD^* = \operatorname{tg}^2\left(\frac{1}{4}\pi+\frac{1}{2}\phi^*\right)$$

and therefore

$$R = \operatorname{tg}\left(\frac{1}{4}\pi+\frac{1}{2}\phi^*\right)\operatorname{tg}\left(\frac{1}{4}\pi+\frac{1}{2}\phi^*-\theta\right) = \frac{\cos\theta+\sin(\phi^*-\theta)}{\cos\theta-\sin(\phi^*-\theta)}.$$

Introduction in Eq. (1.18) gives the relation between ϕ^* and φ to be

$$\sin\varphi = \sin(\phi^*-\theta)/\cos\theta. \tag{1.27}$$

In literature a dilatation angle ν, in the plane strain case, is often defined by $\sin\nu = (\dot{\varepsilon}_1+\dot{\varepsilon}_3)/(-\dot{\varepsilon}_1+\dot{\varepsilon}_3)$. When a sample deforms noncoaxially and this is not noticed by an observer, he will mistake the linear strains $\dot{\varepsilon}(\sigma_1')\dot{\varepsilon}(\sigma_3')$ in the principal stress directions for the principal strain rates $\dot{\varepsilon}_1$, $\dot{\varepsilon}_3$. Instead of ν he will then compute an angle ν^* defined by

$$\sin\nu^* = [\dot{\varepsilon}(\sigma_1')+\dot{\varepsilon}(\sigma_3')]/[-\dot{\varepsilon}(\sigma_1')+\dot{\varepsilon}(\sigma_3')],$$

which, by use of Eqs. (1.26), equals, in the case that $\psi = \frac{1}{2}\pi$,

$$\sin\nu^* = \frac{V_{x,x}+V_{y,y}}{V_{x,x}+V_{y,y}}$$

and with Eqs. (1.22) and (1.25)

$$\sin\nu^* = \sin\theta/\cos(\phi^*-\theta). \tag{1.28}$$

Actually this angle ν^* turns out to be a convenient quantity to introduce, being a constant for this model, independent of the ratio (a^*/b^*).

The system of four equations, Eqs. (1.21) and (1.24), are the basic relations describing the flow mechanism of the double sliding, free rotating model in the case of dilatancy. They express the scalars a^*, b^* (the magnitudes of the shear strain rates) and Ω (the structural rotation) in terms of the components of the velocity gradient tensor. For a^*, b^* the same restriction holds as expressed by the inequalities (1.2) for a, b, because in the case of dilatancy the thermodynamic requirement of energy dissipation must be satisfied. Together with the inequality (1.4) they form the constitutive relations of the dilatant model.

The values of ϕ^* and θ in the basic relations can be determined from φ, the angle of current maximum stress obliquity, and ν^* the angle of dilatation computed from the

linear strain rates in principal stress directions using Eqs. (1.27) and (1.28). These relations are developed here for $\psi = \frac{1}{2}\pi$, but they are invariants, being independent of the orientation of the x, y-coordinates.

2. Character of basic constitutive relations

2.1. System consisting of two inequalities and one equality

The basic relations describing the flow rule of the double sliding, free rotating model are developed in Sect. 1.2. They consist of the four equations Eqs. (1.13) and (1.14), expressing a, b, Ω and change of volume in terms of the components of the velocity gradient tensor. This is a system of four equations relating the two velocity components V_x, V_y and the scalar a, b, Ω, all being five unknowns. Repeated here these relations are

$$
\begin{aligned}
a\sin 2\phi &= +(V_{x,x}-V_{y,y})\sin(2\psi+\phi)-(V_{x,y}+V_{y,x})\cos(2\psi+\phi),\\
b\sin 2\phi &= -(V_{x,x}-V_{y,y})\sin(2\psi-\phi)+(V_{x,y}+V_{y,x})\cos(2\psi-\phi),\\
2\Omega\sin\phi &= +(V_{x,x}-V_{y,y})\sin 2\psi-(V_{x,y}+V_{y,x})\cos 2\psi+(-V_{x,y}+V_{y,x})\sin\phi,\\
V_{x,x}+V_{y,y} &= 0.
\end{aligned}
\tag{2.1}
$$

This system was reduced by several investigators to two equations in the two unknowns V_x, V_y by different additional restrictions imposed of the kinematic behaviour. This generally leads to two partial differential equations on a hyperbolic character. All proposed models agree in the adoption of Eq. $(2.1)_4$ because that equation expresses the fact that volume is conserved during flow. The second equation is obtained by introducing different kinds of limitations.

A *coaxial model* is generated by requiring the two shear strain rates a, b to be equal. Then the second equation becomes Eq. $(2.1)_1$–Eq. $(2.1)_2 = 0$. In that case the characteristics are the bisectrices of the major and minor principal stresses and these are no-extension lines.

In the *non-free rotating model* the structural rotation has a known magnitude, related e.g. to the rotation of principal stress axes. The second equation then consists of Eq. $(2.1)_3$ equated to that known quantity. The characteristics then coincide with the stress characteristics, and are lines along which the relative velocity has the direction of the conjugate characteristic.

In the *single sliding model* the second equation is obtained by requiring either a or b to be zero. This results in two different possibilities. Either Eq. $(2.1)_1 = 0$ or Eq. $(2.1)_2 = 0$. In the first case the characteristics are s^2, t^1 and in the second case s^1, t^2, where t^1 and t^2 are perpendicular to s^2 and s^1, respectively (see Fig. 8). In either case the characteristics are no-extension lines.

In the *double sliding, free rotating model* the structural rotation Ω is not restricted. This is expressed by the inequality (1.4) which implies that the relation $(2.1)_3$ contributes no valuable information being an undetermined part of the constitutive relations in a point.

As useful part there remain only the two relations for the shear strain rates a, b which by the thermodynamic requirement of energy dissipation expressed by the inequality (1.2) obtain the form Eq. $(2.1)_1 \geqq 0$, Eq. $(2.1)_2 \geqq 0$.

The flow rule for the double sliding, free rotating model finally consists of the following system of constitutive relations:

$$
\begin{aligned}
&+(V_{x,x}-V_{y,y})\sin(2\psi+\phi)-(V_{x,y}+V_{y,x})\cos(2\psi+\phi) \geqq 0,\\
&-(V_{x,x}-V_{y,y})\sin(2\psi-\phi)+(V_{x,y}+V_{y,x})\cos(2\psi-\phi) \geqq 0,\\
&(V_{x,x}+V_{y,y}) = 0.
\end{aligned}
\tag{2.2}
$$

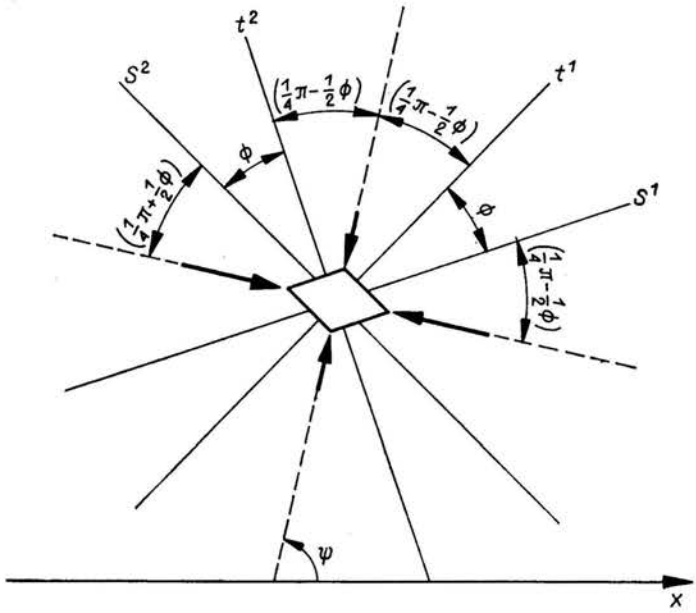

FIG. 8. Directions of $S^1\, t^1\, t^2\, S^2$ with respect to principal stresses.

For solving boundary value problems this is an unusual set, because it contains inequalities and consists of three relations to be satisfied. As a system it cannot be considered to be hyperbolic with characteristic directions. It possesses, however, certain properties resembling those of hyperbolic systems and by using these properties the study of boundary value problems is facilitated.

2.2. Four properties

The first property is, that the system of partial differential relations can be written as an equation containing a total derivative of the velocity components in a particular direction.

The second property is, that the relative velocity of two points on a line has a known direction. If perpendicular to the line, this line conserves length and is a no-extension line.

The third property is, that solving boundary value problems proceeds conveniently if executed in particular directions.

The fourth property is, that strong discontinuities in the velocity can occur in particular directions.

In the case of a linear hyperbolic system of partial differential equations all four properties are possessed by the same lines, the characteristics which are oriented in discrete directions. In the case encountered here different lines possess different properties and their directions are not discrete but can vary within certain regions.

2.3. Multiplicators

In order to investigate this special character and establish the solution procedure it is useful to introduce multiplicators α, β. These are constants independent of x, y and defined in terms of an auxiliary angle j by

$$\alpha = \cos(2j+\phi); \quad \beta = \cos(2j-\phi). \tag{2.3}$$

Depending on the value of j the multiplicators are positive, negative or zero. Since they become separately zero for four different values of j, there are four intervals numbered (1) to (4) each containing a different combination of positive and negative values for α and β. The values of j separating these intervals are those that make either α or β zero and these are numbered according to the intervals they separate. We have with k an integer

$$\begin{aligned}
j_{12}+k\pi &= \frac{1}{4}\pi-\frac{1}{2}\phi, \quad \text{then} \quad \alpha = 0, \quad \beta > 0,\\
j_{23}+k\pi &= \frac{1}{4}\pi+\frac{1}{2}\phi, \quad \text{then} \quad \alpha < 0, \quad \beta = 0,\\
j_{34}+k\pi &= \frac{3}{4}\pi-\frac{1}{2}\phi, \quad \text{then} \quad \alpha = 0, \quad \beta < 0,\\
j_{41}+k\pi &= \frac{3}{4}\pi+\frac{1}{2}\phi, \quad \text{then} \quad \alpha > 0, \quad \beta = 0.
\end{aligned} \tag{2.4}$$

In the intervals separated by these values of j the multiplicators α, β form the following sign combinations:

$$\begin{aligned}
&\text{Interval (1)} \quad -\frac{1}{4}\pi+\frac{1}{2}\phi < (j+k\pi) < \frac{1}{4}\pi-\frac{1}{2}\phi, \quad \text{then} \quad \alpha > 0, \quad \beta > 0,\\
&\text{Interval (2)} \quad \frac{1}{4}\pi-\frac{1}{2}\phi < (j+k\pi) < \frac{1}{4}\pi+\frac{1}{2}\phi, \quad \text{then} \quad \alpha < 0, \quad \beta > 0,\\
&\text{Interval (3)} \quad \frac{1}{4}\pi+\frac{1}{2}\phi < (j+k\pi) < \frac{3}{4}\pi-\frac{1}{2}\phi, \quad \text{then} \quad \alpha < 0, \quad \beta < 0,\\
&\text{Interval (4)} \quad \frac{3}{4}\pi-\frac{1}{2}\phi < (j+k\pi) < \frac{3}{4}\pi+\frac{1}{2}\phi, \quad \text{then} \quad \alpha > 0, \quad \beta < 0.
\end{aligned} \tag{2.5}$$

The multiplicators α, β are used in connection with the shear strain rates a, b to form a quantity c defined by

$$2c = \alpha a+\beta b. \tag{2.6}$$

If no sliding occurs at all, both shear strain rates a and b are zero, and then c vanishes. In that case there is no internal deformation. Let us exclude this case and consider only the situation that either $a > 0$ or $b > 0$ or both $a > 0$ and $b > 0$. Negative values of a and b are not admitted on account of the thermodynamic requirement of energy dissipation as formulated in Eq. (1.2). Then, according to Eqs. (2.4) and (2.5) the following restrictions exist with respect to the sign of c:

(2.7)
$$\begin{aligned}
&\text{in Interval (1)} && c > 0\\
&\text{for } j = j_{12} && c \geqq 0,\\
&\text{in Interval (2)} && c \text{ is unlimited}\\
&\text{for } j = j_{23} && c \leqq 0,\\
&\text{in Interval (3)} && c < 0\\
&\text{for } j = j_{34} && c \leqq 0,\\
&\text{in Interval (4)} && c \text{ is unlimited}\\
&\text{for } j = j_{41} && c \geqq 0.
\end{aligned}$$

2.4. Specific length increase

The quantity c defined by Eq. (2.6) represents specific length increase of lines oriented in particular directions. This can be shown by the following analysis. Using Eqs. $(2.1)_1$ and $(2.1)_2$ in Eq. (2.6) gives with Eq. (2.3)

$$2c = (V_{x,x} - V_{y,y})\cos(2\psi + 2j) + (V_{x,y} + V_{y,x})\sin(2\psi + 2j).$$

Adding Eq. $(2.2)_3$ gives

(2.8)
$$c = V_{x,x}\cos^2(\psi + j) + V_{x,y}\cos(\psi + j)\sin(\psi + j) + V_{y,x}\sin(\psi + j)\cos(\psi + j) + V_{y,y}\sin^2(\psi + j).$$

Let us introduce orthogonal coordinates r^1, r^2 that deviate by the angle j from the principal stress directions such that the angle between r^1 and x is $(\psi + j)$ and the angle between r^2 and x is $\left(\psi + j + \frac{1}{2}\pi\right)$ (see Fig. 9). When ϱ_1, ϱ_3 are the scale parameters, the Jacobi matrix has such coefficients:

(2.9)
$$\begin{aligned}
(\partial x/\partial r^1) &= \varrho_1\cos(\psi + j), & (\partial y/\partial r^1) &= \varrho_1\sin(\psi + j),\\
(\partial x/\partial r^2) &= -\varrho_1\sin(\psi + j), & (\partial y/\partial r^2) &= \varrho_2\cos(\psi + j),\\
(\partial r^1/\partial x) &= (1/\varrho_1)\cos(\psi + j), & (\partial r^2/\partial x) &= -(1/\varrho_2)\sin(\psi + j),\\
(\partial r^1/\partial y) &= (1/\varrho_1)\sin(\psi + j), & (\partial r^2/\partial y) &= (1/\varrho_2)\cos(\psi + j).
\end{aligned}$$

Introduced into Eq. (2.8), this relation becomes with V_p replaced by V^p

$$c = V^p_{,q}(\partial r^1/\partial x^p)(\partial x^q/\partial r^1).$$

The transition from V_p to V^p is allowed because x, y is Cartesian. Indicating velocity components in the r^1, r^2 system by a tilde, this becomes

(2.10)
$$c = \tilde{V}^1_{,1}.$$

The expression (2.10) has the physical interpretation that c represents the specific length increase of a line oriented along r^1. The direction of r^1 is given by its angle j with the minor principal compression stress. The intervals of j and the separation values given by Eqs. (2.4) and (2.5) can therefore be interpreted in terms of directions of r^1. Subsequently the restrictions imposed on c, corresponding to these values of j as given by Eqs. (2.7), can be translated into restrictions on the specific length increase of lines in the r^1-direction. These restrictions can be formulated as follows:

(2.11)
in Interval (1): a line must elongate,
for $j = j_{12}$: a line elongates or conserves length,
in Interval (2): a line elongates, shortens or keeps length,
for $j = j_{23}$: a line shortens or conserves length,
in Interval (3): a line must shorten,
for $j = j_{34}$: a line shortens or conserves length,
in Interval (4): a line shortens, elongates or keeps length,
for $j = j_{41}$: a line elongates or conserves length.

By the choice that the angle j is measured from the minor principal compression stress direction as shown in Fig. 9, the respective intervals are oriented with respect to the principal stress directions as demonstrated in Fig. 10. By comparing $(\psi + j)$ for the separation values j_{12}, ... etc. between intervals as given by Eqs. (2.4) with the values of α_1, α_2 given by Eqs. (1.1) for the stress characteristics, it follows that the separation lines correspond to the stress characteristics s^1, s^2 and the lines t^1, t^2 perpendicular to them in the following manner:

(2.12)
t^2(perpendicular to s^1) has direction j_{12},
stress characteristic s^2 has direction j_{23},
stress characteristic s^1 has direction j_{34},
t^1 (perpendicular to s^2) has direction j_{41}.

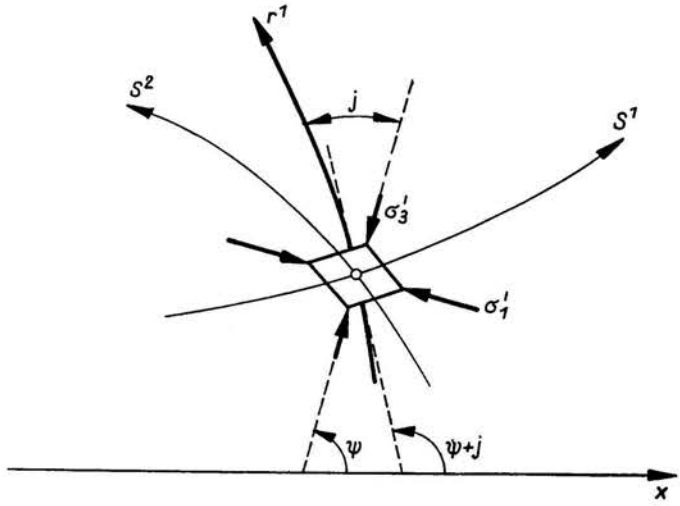

FIG. 9. Direction of r^1 with respect to principal stresses.

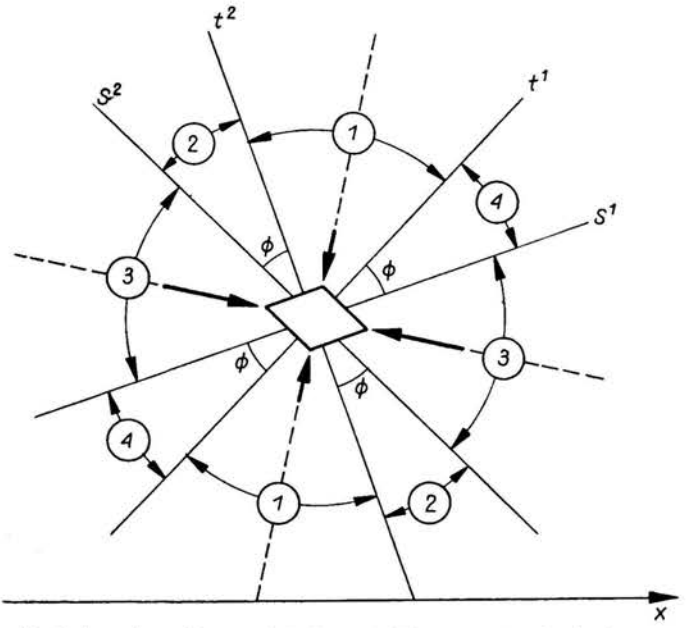

FIG. 10. Orientation of intervals 1, 2, 3, 4 with respect to principal stresses.

As a consequence of the conditions (2.11) and (2.12) it can be stated that

(2.13)
lines between s^1 and s^2 must shorten,
lines between t^1 and t^2 must elongate,
a line along s^1 or s^2 shortens or conserves length,
a line along t^1 or t^2 elongates or conserves length,
lines between s^1 and t^1, or between t^2 and s^2,
either elongate, shorten or conserve length.

2.5. Length conserving lines and acceptable boundary conditions

When the shear strain rates a, b are both zero, then c vanishes according to Eq. (2.6) for all combinations of α, β, this means for all values of j and therefore all possible orientations of r^1. As a consequence every line in the body, whatever its orientation, then conserves its length and this corresponds to a rigid body motion. In that case there is no internal deformation, but there can be rotation.

When only one of the two shear strain rates is zero, for instance $b = 0$ but $a > 0$ such that there is sliding in the s^1-direction, then the value of c vanishes in the two particular directions j_{12} and j_{34} because there, according to Eqs. (2.4), the values of α is zero. This means that there exist two lines for which c vanishes, indicating that the length of these lines does not change during flow. These no-extension lines are perpendicular, and this agrees with the condition of no volume change. The length conserving lines in this case are, according to the relations (2.12)

for j_{34} the stress characteristic s^1,
for j_{12} the t^2-line perpendicular to s^1.

When there is only sliding along the s^2-directions, such that $a = 0$ and $b > 0$, then c is zero for j_{23} and j_{41}. In that case the length conserving lines are the stress characteristic s^2 and the line t^1 perpendicular to s^2.

When both slidings occur, such that $a > 0$, $b > 0$, then c vanishes for values of j where α and β have different signs. This is so according to the inequalities (2.5) in Intervals (2) and (4). In that case the length conserving lines are two perpendicular lines, one in Interval (2), the other in Interval (4).

The restrictions (2.11) imposed on length change of lines have to be obeyed by boundary conditions, for being acceptable. Let a boundary value problem consist of a given limit stress state in a body and a velocity distribution imposed on the boundary. When the boundary has an angle μ with the x-axis, the boundary can be conceived as a line r^1 at an angle $j = \psi - \mu$ with the minor principal compression stress. The value of j determines by the inequalities (2.5) the interval in which the boundary is located.

When the boundary lies in Interval (1), the velocity distribution along it must elongate the boundary line. When lying in Interval (3), the boundary line must shorten. If the boundary motions are such that its length is conserved, then internal deformation and strain rate can only occur when the boundary is located in Intervals (2) or (4). If not, the adjacent body has to remain undeformed and only executes rigid body motions.

A velocity distribution can only constitute an acceptable boundary condition if these restrictions are not violated.

2.6. Construction of a velocity distribution

In order to construct velocity distributions from boundary conditions, the relation (2.10) can be used, either for a mathematical integration procedure or a graphical construction in the hodograph plane.

The mathematical elaboration requires to convert the covariant derivative of the relation (2.10) into a partial derivative. This can be done be using the rule for covariant differentiation which in this case leads to

$$c = \tilde{V}^1_{.1} = (\partial \tilde{V}^1/\partial r^1) + \Gamma^1_{1m} \tilde{V}_m. \tag{2.14}$$

The Christoffel symbols in this expression can be found by using the rule

$$\Gamma^k_{lm} = \frac{\partial r^k}{\partial x^\alpha} \frac{\partial^2 x^\alpha}{\partial r^l \partial r^m},$$

which, applied to the coefficients expressed by Eqs. (2.9), gives

$$\Gamma^1_{11} = (1/\varrho_1)(\partial \varrho_1/\partial r^1),$$
$$\Gamma^1_{12} = -(\varrho_2/\varrho_1)[\partial(\psi + j)/\partial r^1].$$

So Eq. (2.14) becomes

$$c = \frac{\partial(\varrho_1 \tilde{V}^1)}{\varrho_1 \partial r^1} - (\varrho_2 \tilde{V}^2) \frac{\partial(\psi + j)}{\varrho_1 \partial r^1}. \tag{2.15}$$

In this expression $\varrho_1 \tilde{V}^1$, $\varrho_2 \tilde{V}^2$ are the physical velocity components in the r^1, r^2 coordinate directions. Since further on only differentials in the r^1-direction are involved, it is possible

to integrate Eq. (2.15), if the magnitude of c is known. However, only the sign of c is known and therefore the solution consists of bounds limiting possible velocity distributions. Representation of these bounds in mathematical terms is somewhat intricate; better suited for comprehension is to express them graphically.

The graphical procedure consists in constructing the above mentioned bounds in a hodograph plane. Every point P in the physical x, y-plane has an image P' in the hodograph plane such that the coordinates of P' are the components of the velocity V_P of P. The vector $P'Q'$ in the hodograph plane is the vector representing the relative velocity $(V_Q - V_P)$ of the point Q with respect to the point P (see Fig. 11).

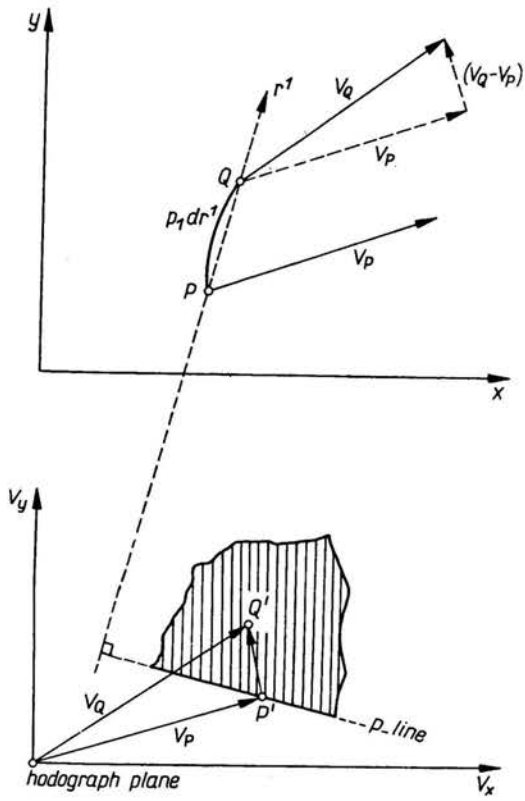

FIG. 11. Points P', Q' in hodograph plane represent velocities V_P, V_Q of point P, Q in x, y-plane.

When Q is located on a r^1-line through P at a distance of magnitude $\varrho_1 dr^1$, the relative velocity of Q with respect to P has components of magnitude $\varrho_1 \tilde{V}^1_{.1} dr^1$, $\varrho_2 \tilde{V}^2_{.1} dr^1$ in r^1, r^2 directions respectively. From the relation (2.10) it can be concluded that the r^1-component is $\varrho_1 c\, dr^1$ and therefore positive, negative or undetermined depending on the interval corresponding to the direction of r^1 and the conditions (2.7) imposed on c by that interval.

When r^1 is oriented in Interval (1), c is positive and the line PQ elongates. In the hodograph, (see Fig. 11), this means that the location of Q' is limited to a half space. This half space is bounded by the line p through P' perpendicular to the chord of PQ. The region

for Q' (shaded in Fig. 11) is on the side of p, corresponding to the side occupied by the endpoint Q on the line PQ. When r^1 is oriented such as to lie in Interval (3), c is negative and the location of Q' is limited to the half space bound by the same line p, but on the other side. These considerations indicate how to construct the range of velocities possible in a point of the xy-plane by limiting the region in the hodograph where its image is allowed to lie. Because of the conditions (2.7) only lines r^1 in Intervals (1) and (3) can contribute valuable information in this respect.

The construction in the hodograph plane consists in locating the image of a point in such a manner that the conditions imposed on the sign of c are satisfied. However, this is not yet sufficient to guarantee that both shear strain rates a, b are positive, separately. This can be shown by considering an arbitrary line in Interval (1) where, according to the inequalities (2.5), both α and β are positive. Introduced in (2.6) the requirements (1.2) on a and b show that it is necessary for c to be positive. However, a positive value for c means only that

$$\alpha a+\beta b \geqq 0,$$

which is an inequality that can be written in the two following alternative ways:

$$a \geqq -\beta b/\alpha \quad \text{or} \quad b \geqq -\alpha a/\beta.$$

The first shows that a can be negative for positive b and the second that b can be negative for positive a.

This shows that a construction in the hodograph, satisfying $c \geqq 0$ for a line in Interval (1), is not yet sufficient. In order to guarantee that both a and b are positive separately, it is necessary to execute two analyses in Interval (1), which will be indicated by t_1 and t_2 respectively here, because they involve the lines t^1 and t_2.

Analysis t^1. By choosing r^1 to be oriented along a t^1-line, the value of j is, according to the relations (2.12), equal to j_{41} and, according to Eqs. (2.4), we then have $\alpha > 0$, and $\beta = 0$. Since then $c = \alpha a$, it is enough to require $c \geqq 0$ in order to guarantee that a is positive.

Analysis t^2. By choosing r^1 to be oriented along a t^2-line, the value of j is, according to (2.12), equal to j_{12} and, according to Eqs. (2.4), we then have $\alpha = 0$, and $\beta > 0$. Since then $c = \beta b$, it is enough to require $c \geqq 0$ in order tn guarantee that b is positive.

The same can be done in Interval (3) where c must be negative. The two required analyses are called s^1, s^2.

Analysis s^1. Choose $j = j_{34}$, then $\alpha = 0$, $\beta < 0$ and by requiring $c \leqq 0$ it is guaranteed that b is positive.

Analysis s^2. Choose $j = j_{23}$, then $\alpha < 0$, $\beta = 0$ and by requiring $c \leqq 0$ it is guaranteed that a is positive.

Graphically the four analyses t^1, t^2, s^1, s^2 result in the drawing of four boundary lines in the hodograph. Let us consider the problem to determine the velocity in a point C of the x, y-plane when the velocities are known in four points A, D, E, B, which are connected to C by a s^1, t^1, t^2, s^2-line, respectively (see upper part of Fig. 12). These four velocities are represented in the hodograph by the four image points A', D', E', B'.

The analysis consists in drawing lines a, d, e, b in the hodograph plane, perpendicular

respectively to the chords of the lines AC, DC, EC, BC in the x, y-plane. In order to satisfy the conditions (2.7), the possible location for C' in the hodograph is the shaded area in Fig. 12 enclosed by the lines a, d, e, b.

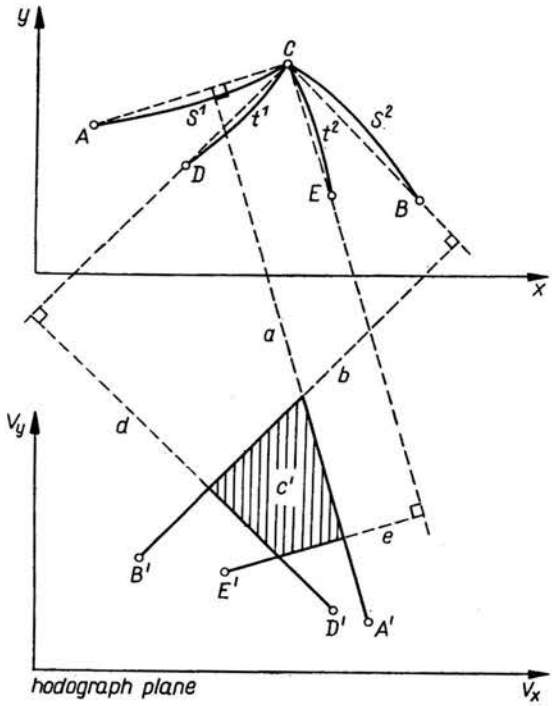

FIG. 12. Region for C' in hodograph plane constructed from points A', B', D', E' representing the velocities of A, B, D, E in x, y-plane.

2.7. Characteristic properties

From the properties listed in Sect. 2.2 and possessed by characteristics of hyperbolic systems, the first three are related to the results obtained in this chapter.

Whether the first property is possessed by the system can be verified by considering the relation $c = \tilde{V}^1_{,1}$, given by Eq. (2.10). In developing from it the expression (2.15), it was shown to consist of partial derivatives with respect to r^1 only. Since r^1 can have any direction, it is therefore possible to develop an expression in terms of a total derivative in any desired direction. However, the expressions obtained do not have the character of an equation because the value of c is unknown. Depending on the direction of r^1, only its sign is known as given by (2.7). Therefore, the expression (2.15) is not an equation but essentially an inequality. There are regions for r^1 though, where c can be zero, and Eq. (2.15) becomes an equation. As shown by (2.11) and (2.12) these regions are limited to Interval (2) with its separation lines s^2 and t^2, and Interval (4) with its separation lines s^1 and t^1.

The second property can be verified by (2.11), which shows by (2.12), that length conserving lines are limited to Interval (2) with its separation lines s^2 and t^2 and Interval (4) with its separation lines s^1 and t^1.

The third property is related to the analysis in Sect. 2.6. It was shown that the construction of velocity distributions most conveniently proceeds along the lines $t^1\,t^2\,s^1\,s^2$.

So far the conclusion of the analysis may be that Interval (4) with its boundary lines $s^1\,t^1$ and Interval (2) with its boundary lines $s^2\,t^2$, are comparable to two conjugate characteristics. Since the intervals have as aperture of magnitude ϕ (see Fig. 10), their aperture reduces to zero in perfect plasticity when $\phi = 0$. The boundary lines $s^1\,t^1$ ten reduce to one characteristic and the boundaries $s^2\,t^2$ to the conjugate characteristic, with properties known to exist in perfect plasticity.

2.8. Dilatancy

The considerations developed in this chapter can be used in the same manner for the case of dilatancy. The system of relations (2.2) basic to the model, then becomes by using Eqs. $(1.21)_1$, $(1.21)_2$ and (1.24)

$$
\begin{aligned}
&(V_{x,x}-V_{y,y})\sin(2\psi+\phi^*-\theta)-(V_{x,y}+V_{y,x})\cos(2\psi+\phi^*-\theta) \geqq 0,\\
&-(V_{x,x}-V_{y,y})\sin(2\psi-\phi^*+\theta)+(V_{x,y}+V_{x,y})\cos(2\psi-\phi^*+\theta) \geqq 0,\\
&(V_{x,x}+V_{y,y})\cos(\phi^*-\theta)-(V_{x,x}-V_{y,y})\cos 2\psi\sin\theta+(V_{x,y}+V_{y,x})\sin 2\psi\sin\theta = 0.
\end{aligned}
\tag{2.16}
$$

In order to reproduce the subsequent analysis it is necessary to introduce multiplicators α^*, β^* of the form

$$
\alpha^* = \cos(2j+\phi^*-\theta)+\sin\theta, \qquad \beta^* = \cos(2j-\phi^*+\theta)+\sin\theta. \tag{2.17}
$$

The quantity c^* defined by

$$
2c^* = \alpha^* a^* + \beta^* b^*, \tag{2.18}
$$

then becomes with Eqs. $(1.21)_1$, $(1.21)_2$ and (1.24)

$$
2c^* = (V_{x,x}+V_{y,y})+(V_{x,x}-V_{y,y})\cos(2\psi+2j)+(V_{x,y}+V_{y,x})\sin(2\psi+2j) \tag{2.19}
$$

and this shows by the analysis following Eq. (2.8) that also c^* represents specific length increase of lines at an angle j with the minor principal compression stress.

The intervals corresponding to positive, negative and unlimited values of c^* are now given by

$$
\begin{aligned}
&\text{Interval (1)} && -\frac{1}{4}\pi+\frac{1}{2}\phi^*-\theta < (j+k\pi) < \frac{1}{4}\pi-\frac{1}{2}\phi^*+\theta,\\
&\text{Interval (2)} && \frac{1}{4}\pi-\frac{1}{2}\phi^*+\theta < (j+k\pi) < \frac{1}{4}\pi+\frac{1}{2}\phi^*,\\
&\text{Interval (3)} && \frac{1}{4}\pi+\frac{1}{2}\phi^* < (j+k\pi) < \frac{3}{4}\pi-\frac{1}{2}\phi^*,\\
&\text{Interval (4)} && \frac{3}{4}\pi-\frac{1}{2}\phi^* < (j+k\pi) < \frac{3}{4}\pi+\frac{1}{2}\phi^*-\theta.
\end{aligned}
\tag{2.20}
$$

By choosing j to be measured from the minor principal compression stress direction, the separation lines between intervals are in analogy to (2.12) s^{1*}, s^{2*} and t^{1*}, t^{2*} with the following specifications (Fig. 13). The lines s^{1*} and s^{2*} coincide with the average directions of the conjugate sliding planes, the lines t^{1*} and t^{2*} deviate from them by an angle of

magnitude $(\phi^*-\theta)$ and are perpendicular to the surfaces of the steps along which sliding occurs. When there is only sliding along s^1*-planes, such that $b^* = 0$, the length conserving lines are s^{1*} and t^{2*}. Similarly, when $a^* = 0$ the length conserving lines are s^{2*} and t^{1*}. The lines in these pairs deviate by an angle $\left(\frac{1}{2}\pi+\theta\right)$.

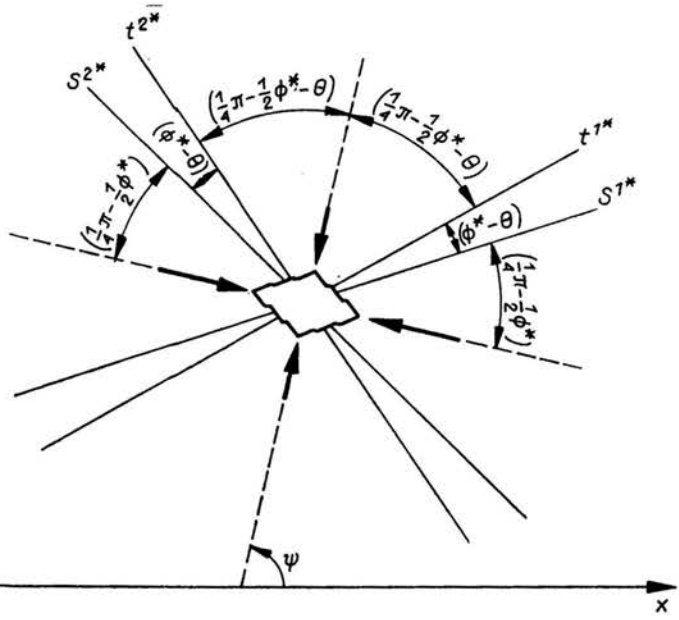

FIG. 13. Directions of s^1, t^1, t^2, s^2 with respect to principal stresses in the case of dilatancy.

For constructing velocity distributions from boundary conditions the lines $s^{1*}s^{2*}t^{1*}$ t^{2*} have the same function as explained for $s^1s^2t^1t^2$ in Sect. 2.6.

3. Discontinuities

3.1. Strong velocity discontinuity as the limit of homogeneous shear strain rate

The flow rule of the double sliding, free rotating model is expressed by Eqs. (2.2) in terms of the components of the velocity gradient tensor $V_{x,x}, V_{x,y}, V_{y,x}, V_{y,y}$. These components are finite quantities when the velocity distribution is continuous. In reality the motion is not necessarily restricted to continuous distributions, but also discontinuities can occur. If the discontinuity is in the velocity itself, it is called a strong discontinuity and in that case one or several of the components of the velocity gradient tensor become infinitely large.

In order to investigate the strong discontinuities that are implied by the mathematical formulation of the model behaviour, such a discontinuity will be developed here from a continuous velocity distribution in and around a thin band. In the band the velocity changes gradually between two values whose difference is the relative velocity of the two regions

bordering the band on either side. When the band has a finite thickness the shear strain rate within the band is also finite. When the relative velocity is kept constant and the thickness of the band is reduced, the shear strain rate increases within the band. This shear strain rate becomes infinite in the limit that the band thickness is reduced to zero. Then a strong velocity discontinuity is created.

Let the band be straight and possess a thickness h and an inclination μ with the x-axis (Fig. 14). Coordinates ξ, η are introduced parallel and perpendicular to the band. The band occupies the region $0 \leqq \eta \leqq h$ and has a constant thickness in the ξ-direction. The material below the band is at rest and, above, the material moves as a rigid block with velocity ΔV parallel to the band. Expressed mathematically this is

$$\begin{aligned} V_\xi &= 0, \quad V_\eta = 0 \quad \text{for} \quad \eta \leqq 0, \\ V_\xi &= \Delta V, \quad V_\eta = 0 \quad \text{for} \quad \eta \geqq 0. \end{aligned} \tag{3.1}$$

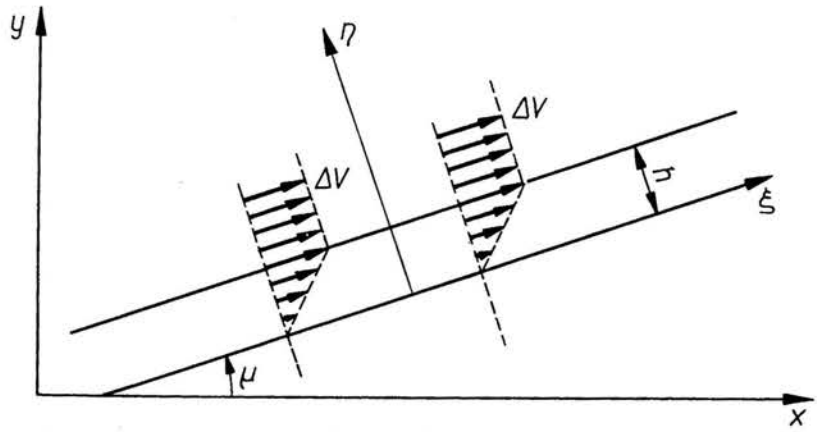

FIG. 14. Two rigid regions, moving at a velocity ΔV with respect to each other and separated by a thin band with a gradual velocity increase from 0 to ΔV.

The velocities within the band are assumed to be distributed linearly and to consist only of velocities parallel to the band such that

$$V_\xi = \Delta V \frac{\eta}{h}, \quad V_\eta = 0 \quad \text{for} \quad 0 \leqq \eta \leqq h. \tag{3.2}$$

The velocity distribution given by Eqs. (3.1) and (3.2) is everywhere continuous and therefore the components of the velocity gradient tensor are finite. In the band a strain rate of the character of a simple shear exists with a magnitude m defined by

$$m = \Delta V/h.$$

The value of m becomes infinite when h reduces to zero, while ΔV keeps a fixed, finite value.

3.2. Possible directions of strong velocity discontinuity

In order to investigate the directions in which such a band can occur, the motion described by Eq. (3.2) is translated in terms of the x, y-components of the velocity gradient tensor. Possible directions are then found by determining the values of μ which satisfy

the constitutive relations (2.2). Transition from ξ, η to x, y-coordinates gives for Eq. (3.2) with Fig. 14

$$\begin{aligned} V_x &= V_\xi \cos\mu = m\eta\cos\mu, \\ V_y &= V_\xi \sin\mu = m\eta\sin\mu \end{aligned} \qquad \text{for} \quad 0 \leqq \eta \leqq h.$$

The x, y-components of the velocity gradient tensor are obtained by differentiation with respect to x, y. This gives by using the chain rule and the relations (see Fig. 14)

$$\partial\eta/\partial x = -\sin\mu, \qquad \partial\eta/\partial y = \cos\mu,$$

the following values:

$$\begin{aligned} V_{x,x} &= m\cos\mu\,\frac{\partial\eta}{\partial x} = -m\cos\mu\sin\mu, \\ V_{x,y} &= m\cos\mu\,\frac{\partial\eta}{\partial y} = m\cos^2\mu, \\ V_{y,x} &= m\sin\mu\,\frac{\partial\eta}{\partial x} = -m\sin^2\mu, \\ V_{y,y} &= m\sin\mu\,\frac{\partial\eta}{\partial y} = m\sin\mu\cos\mu. \end{aligned} \tag{3.3}$$

Introduction of these values in Eq. $(2.2)_3$ shows that equation is satisfied identically, ensuring conservation of volume; introduction in Eqs. $(2.2)_1$ and $(2.2)_2$ shows that the requirements imposed by the flow rule reduce to

$$\begin{aligned} -m\cos(2\psi+\phi-2\mu) &\geqq 0, \\ m\cos(2\psi-\phi-2\mu) &\geqq 0. \end{aligned} \tag{3.4}$$

The relations (3.4) define two admissible regions for μ depending on the sign of m:

Identyfing a strong discontinuity, at an angle μ, with a line r^1, at an angle j with the principle stress directions as shown in Fig. 9, we have

$$\mu = \psi + j.$$

Comparison with the inequality (2.5) and Fig. 10 shows that

$$\begin{aligned} &m > 0 \text{ corresponds to Interval (4) between } s^1 \text{ and } t^1, \\ &m < 0 \text{ corresponds to Interval (2) between } t^2 \text{ and } s^2. \end{aligned} \tag{3.5}$$

From this analysis it follows that possible directions for strong discontinuities are located in Intervals (4) and (2) with their boundaries s^1, t^1 and t^2, s^2 included.

The fourth property listed in Sect. 2.2 therefore has the same character as the other three properties, leading to the conclusion that Intervals (4) and (2) with their boundaries possess properties comparable to those of the characteristics in perfect plasticity when $\phi = 0$.

3.3. Kinematic interpretation of strong discontinuities

The velocity distribution considered in Sect. 3.1 and 3.2 consists of a large strain rate within a small band, surrounded by regions that translate as rigid blocks. These blocks were introduced in order to simplify the mathematics, but it is not necessary that they remain

undeformed and only translate. The analysis remains valid also when the adjacent regions deform internally and rotate. The reason is that m, the shear strain rate within the band, tends towards infinity and therefore any finite strain rate or velocity gradient outside the band can be disregarded with respect to m.

There exist, however, limitations on the shear strain rates in the adjacent regions because the band is restricted in its orientation and the lines bordering the band have to satisfy the requirements imposed on lines in the respective regions as formulated in the restrictions (2.11). It may be remarked here that for perfect plasticity, when the intervals collapse, because $\phi = 0$, so that the lines s^1t^1 coincide and the lines t^2s^2 coincide, the requirements (2.11) reduce the resulting lines to no-extension lines. This leads to the well-known property in perfect plasticity which claims that a line adjacent to a strong discontinuity in the velocity always conserves its length. When ϕ is not zero this restriction to conservation of length is no longer imperative.

From the analysis in Sect. 3.2 it follows that a strong discontinuity can have various directions lying between s^1 and t^1 or between t^2 and s^2. From a physical view point only the directions s^1 and s^2 are to be expected, because the model is based on the assumption of sliding motions along those lines exclusively, and each sliding between two slices of finite thickness is in fact a strong velocity discontinuity.

The mathematical formulation of the flow rule, however, admits also strong discontinuities in directions deviating from s^1, s^2 with, in the extreme case, the lines t^1, t^2 perpendicular to s^2, s^1 respectively. In order to investigate the probability of occurrence of those deviating directions, it is necessary to analyze in some detail the kinematics involved. As an example the case of a discontinuity developing along a t^1-line is considered here.

A t^1-line has according to (2.12) a direction j_{41} and so with Eqs. (2.4) we have $\mu = \psi + j = \left(\psi + \frac{3}{4}\pi + \frac{1}{2}\phi\right)$. Introduced in Eqs. (3.3) this gives

$$(V_{x,x} - V_{y,y}) = m\cos(2\psi+\phi), \quad (V_{x,y} + V_{y,x}) = m\sin(2\psi+\phi)$$

and this in Eqs. (1.13) results in

$$a = 0, \quad b = +m, \quad \Omega = -m. \tag{3.6}$$

For a t^1-line m is a positive quantity according to (3.5).

The flow mechanism in Eqs. (3.6) consists of slidings of magnitude m in the s^2-direction, combined with a clockwise structural rotation of the same magnitude. Since t^1 is perpendicular to s^2, this motion requires that the band of large shear strain rate be subdivided into slices perpendicular to the band as shown in Fig. 15, left. The slices slide and rotate to come in position of Fig. 15, middle, with the result that the material above the band moves as a rigid block in a direction parallel to the band.

This kind of motion is called the tilting bookrow mechanism because it is similar to a row of books that topple over when its support on one side is removed. For the motion to develop it is necessary that the material within the band rotates and, considering an individual slice, it is required that both ends be able to rotate with respect to the adjacent material outside the band that only translates. The consequence is that gaps are created

as shown in Fig. 15, middle. By producing the slices in the adjacent material (dashed in Fig. 15, right), they can be visualized as beams that have to bend on either side of the band. The gaps are formed when the beams break.

When the slices are internally strong enough to resist the bending, the tilting bookrow mechanism is prevented to develop and as a consequence strong discontinuities will not occur in directions t^1 or t^2. It is a physical question how much bending resistance the slices are able to supply. In a granular assembly the slices are loosely connected conglomerates of particles, held together only by forces in the contact points. They are flexible units and it is hard to believe that such conglomerates are capable of resisting the formation of hinges, when their length is much larger than their width. It has not yet been established experimentally how many particle diameters the thickness of a band has at least to be for the effect of the tilting bookrow mechanism to develop. It seems that tilting bookrow mechanisms were observed in bands of only a few centimeters thickness.

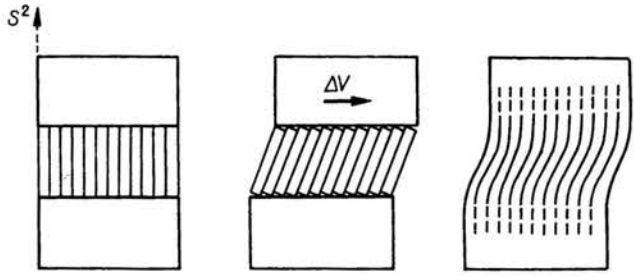

FIG. 15. Slices in S^2 direction, tilting bookrow mechanism and bending of slices.

The conclusion at this point may be that bands, separating regions with a relative velocity parallel to the band, can develop in different directions, if the bandsize is at least a few centimeters thick. For the evaluation of a real situation a few centimeters can be treated mathematically as of zero thickness. As a consequence the mathematical possibility for the occurrence of strong velocity discontinuities in directions deviating from s^1, s^2 must be admitted, if for practical engineering purposes it is required not to overestimate the internal resistance of a grain structure.

4. Conclusions

The flow rule of the double sliding, free rotating model consists of a system of two inequalities and one equality in terms of the four components of the velocity gradient tensor. In fact these components are the partial derivatives with respect to x and y of the two velocity components. The system of two inequalities and one equality, for the two unknown velocity components, forms an unusual set for solving boundary value problems.

The system resembles a set of hyperbolic equations because specific directions can be indicated, possessing particular properties which remind of the properties owned by characteristics. Instead of discrete characteristic lines, however, in this case regions or intervals

of directions are involved. The intervals are separated by four lines: s^1, t^1, t^2, s^2. From these the lines s^1 and s^2 correspond to the sliding planes, and the lines t^1 and t^2 are perpendicular respectively to s^2 and s^1. In the case of dilatancy the s^{1*} and s^{2*} lines correspond to the sliding planes, while t^{1*} and t^{2*} have an angle $\left(\frac{1}{2}\pi+\theta\right)$ with them, being perpendicular to the surfaces of the steps along which sliding occurs.

These specific lines are length conserving lines in the extreme cases, that either $a = 0$ or $b = 0$. When both slidings are active the length conserving lines are located in Intervals (2) and (4), being perpendicular in the case of no volume change and enclosing an angle $\left(\frac{1}{2}\pi+\theta\right)$ in the case of dilatancy.

For determining the velocity in a point C of a region, with a known limit stress state and velocities given on a boundary, it is necessary to consider the s^1, t^1, t^2, s^2 lines through C. The four lines are continued up to points where the velocities are known, giving four starting points in the, hodograph plane. Four lines drawn perpendicular to the chords of the s^1, t^1, t^2, s^2 lines through the respective starting points give a quadrangle in the hodograph. All points within the quadrangle represent a velocity that can be executed by C.

Lines containing strong discontinuities in the velocity are analyzed as the limit of bands containing large strain rates. The mathematical formulation admits the possibility that the bands can be infinitely thin in various directions within Intervals (2) and (4). The physical basis of the model suggests that only in the directions of s^1, s^2 the bands can reduce to thin zones and that in other directions the bands must have a finite thickness, being the largest for bands in the directions of t^1, t^2. The band thickness, however, remains small enough to consider it to be zero for practical purposes.

The double sliding, free rotating model for the flow of granular media in the limit stress state is but a model. The real behaviour of granular particles during flow is intricate, and the simplification of sliding, exclusively along planes corresponding to the planes of exhausted shear resistance, represents this behaviour only partly. However, this part constitutes the major difference between the normal building materials and granular media. A system consisting of discrete and unconnected particles derives its internal resistance from friction, and sliding occurs between individual particles when the friction is exhausted. The simplification of sliding planes incorporates this typical aspect of friction and therefore the kinematics of the model exemplifies the anomalous behaviour of granular materials.

It was considered of interest to develop consistently the mathematical consequences of the kinematics following from the model in order to understand and possibly predict what real granular media might do.

Acknowledgment

I am indebted to Dr J. OSTROWSKA-MACIEJEWSKA and Dr A. DRESCHER for pointing my attention to misformulations in my previous publications, and to Professor Z. MRÓZ for profounding the model properties with his research group at the Institute of Fundamen-

tal Technological Research, Warsaw. This paper contains the results of the fruitful discussions in 1975 with Dr DRESCHER, who patiently helped me to investigate the particular character of the model in order to develop a more consistent basis for its mathematical description.

References

1. C. A. COULOMB, *Sur une application des règles de maximis et minimis à quelques problèmes de statique relatifs à l'architecture*, Acad. Roy. Sci. Math. Phys. par divers savants, **7**, 343–382, 1773.
2. A. DRESCHER, G. DE JOSSELIN DE JONG, *Photoelastic verification of a mechanical model for the flow of a granular material*, J. Mech. Phys. Solids, **20**, 337–351, 1972.
3. A. DRESCHER, *An experimental investigation of flow rules for granular materials using optically sensitive glass particles*, Geotechnique, **26**, 4, 591–601, 1976.
4. G. A. GENIEV, *Problems of the dynamics of a granular medium* [in Russian], Akad. Stroit. Archit. SSSR, Moscow 1958.
5. G. DE JOSSELIN DE JONG, *The undefiniteness in kinematics for friction materials*, Proc. Conf. Earth Pressure Probl., Brussels, **1**, 55–70, 1958.
6. G. DE JOSSELIN DE JONG, *Statics and kinematics in the failable zone of a granular material*, Thesis, University of Delft 1959.
7. G. DE JOSSELIN DE JONG, *The double sliding, free rotating model for granular assemblies*, Geotechnique, **21**, 2, 155–163, 1971a.
8. G. DE JOSSELIN DE JONG, Discussion in Proc. Roscoe Memorial Symp., *Stress-strain behaviour of soils*, 258–261, Cambridge 1971b.
9. G. DE JOSSELIN DE JONG, *Behaviour of granular materials in progressive flow*, Lecture notes, Int. Centr. Mech. Sciences (CISM), Udine, Italy [in print], 1974.
10. G. DE JOSSELIN DE JONG, *Rowe's stress-dilatancy relation based on friction*, Geotechnique, **25**, 3, 527–534, 1976.
11. J. MANDEL, *Sur les lignes de glissement et le calcul des déplacements dans la déformation plastique*, C. r. hebd. Séanc. Acad. Sci., **225**, 1272–1273, Paris 1947.
12. J. MANDEL, *Sur les équations d écoulement des sols ideaux en déformation plane et le concept du double glissement*, J. Mech. Phys. Solids, **14**, 303–308, 1966.
13. G. MANDL, R. FERNÁNDEZ LUQUE, *Fully developed plastic shear flow of granular materials*, Géotechnique, **20**, 3, 277–307, 1970.
14. Z. MRÓZ, *On stress-strain relations in soil mechanics*, Proc. First Baltic Conf. on Soil Mech. and Found Eng., 126-164, Gdańsk 1975.
15. P. L. NEWLAND, B. H. ALLELY, *Volume changes in drained triaxial tests on granular material*, Geotechnique, **7**, 1, 17–34, 1957.
16. P. W. ROWE, *The stress dilatancy relation for static equilibrium of an assembly of particles in contact*, Proc. Roy. Soc., **A269**, 500–527, 1962.
17. P. W. ROWE, *The relation between the shear strength of sands in triaxial compression, plane strain and direct shear*, Géotechnique, **19**, 1, 75–86, 1969.
18. A. J. M. SPENCER, *A theory of the kinematics of ideal soils under plane strain conditions*, J. Mech. Phys. Solids, **12**, 337–351, 1964.
19. L. S. ZAGAINOV, *On the question of the plane stationary strain of granular medium* [in Russian], Mech. Tverdovo Tela, **2**, 188–196, 1967.

DELFT UNIVERSITY OF TECHNOLOGY
DEPARTMENT OF CIVIL ENGINEERING.

Received December 30, 1976.